Earth and Planetary Science Letters 454 (2016) 55–64

Contents lists available at ScienceDirect

Earth and Planetary Science Letters

www.elsevier.com/locate/epsl

New constraints on the most significant paleointensity change in Western Europe over the last two millennia. A non-dipolar origin?

Miriam Gómez-Paccard [a,*], María Luisa Osete [a,b], Annick Chauvin [c], Francisco J. Pavón-Carrasco [a,b], Manuel Pérez-Asensio [d], Pedro Jiménez [e], Philippe Lanos [c,f]

[a] Instituto de Geociencias (IGEO), CSIC-UCM, Ciudad Universitaria, 28040 Madrid, Spain
[b] Departamento Física de la Tierra I, Facultad de Ciencias Físicas, Universidad Complutense, 28040 Madrid, Spain
[c] Géosciences-Rennes, UMR 6118, CNRS, Université de Rennes 1, Campus de Beaulieu, Bât. 15, CS 74205, 35042 Rennes, France
[d] Freelance archeologist, Granada, Spain
[e] Escuela de Estudios Árabes EEA-CSIC, Frailes de la Victoria, 1810 Granada, Spain
[f] Centre de Recherches en Physique Appliquée à l'Archéologie, UMR 5060, CNRS, Université de Bordeaux 3, France

ARTICLE INFO

Article history:
Received 30 November 2015
Received in revised form 12 July 2016
Accepted 9 August 2016
Available online 6 September 2016
Editor: B. Buffett

Keywords:
archeomagnetism
archeointensity
rapid intensity changes
secular variation
dipole moment
non-dipolar sources

ABSTRACT

Over the last years new evidences of several short-lived regional maxima of the geomagnetic field intensity at various times and locations have been defined. These features have important implications both for geomagnetic field modeling and for Earth's dynamo simulations. However, the nature, extent and underlying causes of these variations are still poorly understood. The major constraint for an adequate description of these important features is the absence of continuous detailed records and the current limited availability of precisely dated geomagnetic field recorders. In this context, archeological materials from superimposed strata covering long sequences of occupation provide a powerful tool to investigate the temporal variability of geomagnetic field strength at decadal and centennial time scales. In this work we report the archeomagnetic study of 79 potteries from Southeastern Spain collected in 14 different stratigraphic units. The chronological framework of the studied collection, ranging from the 9th to the 12th centuries, is based on historical/archeological data such as written sources and well-established typological and archeometric documentation on ceramics found on reference contexts in the area. Additionally, two radiocarbon dates obtained from two different stratigraphic units confirm the proposed chronological intervals. From classical Thellier and Thellier experiments including partial thermoremanent magnetization (pTRM) checks and TRM anisotropy and cooling rate corrections, height new high-quality mean intensities were derived. The new data provide an improved description of the sharp abrupt intensity decay that took place in Western Europe after the 800 AD intensity maximum, the most significant geomagnetic field intensity feature observed in Europe over the last two millennia. The new results confirm that several rapid intensity changes (with rates higher than 10 μT/century) took place in Western Europe during the recent history of the Earth. The comparison between the regional curve of Western Europe and the SHA.DIF.14k global field model predictions suggests that the 800 AD event observed in Europe is probably controlled by non-dipolar geomagnetic sources.

1. Introduction

Recent studies (e.g. Ben-Yosef et al., 2009; de Groot et al., 2013; Ertepinar et al., 2012; Genevey and Gallet, 2002; Gallet et al., 2003; Hervé et al., 2013; Hong et al., 2013; Schnepp et al., 2009; Shaar et al., 2011; Genevey et al., 2009, 2013; Gómez-Paccard et al., 2008, 2012a; Mitra et al., 2013; Cai et al., 2014) corroborate the occurrence of short-lived regional maxima of the geomagnetic field intensity during the last few millennia. A better understanding of the nature and causes of these intriguing phenomena is not only important to understand the processes that govern the Earth's dynamo but also to place into a long-term temporal perspective the current decay of the low field intensity anomaly currently centered around Southern Brazil and Paraguay (the so-called South Atlantic Anomaly, SAA) and the historically observed rapid decay of the dipole moment (of about 5% per century for the last

* Corresponding author.
E-mail addresses: mgomezpaccard@igeo.ucm-csic.es (M. Gómez-Paccard), mlosete@fis.ucm.es (M.L. Osete), annick.chauvin@univ-rennes1.fr (A. Chauvin), manuelperease@yahoo.es (M. Pérez-Asensio), pedro@eea.csic.es (P. Jiménez), philippe.lanos@univ-rennes1.fr (P. Lanos).

http://dx.doi.org/10.1016/j.epsl.2016.08.024
0012-821X/

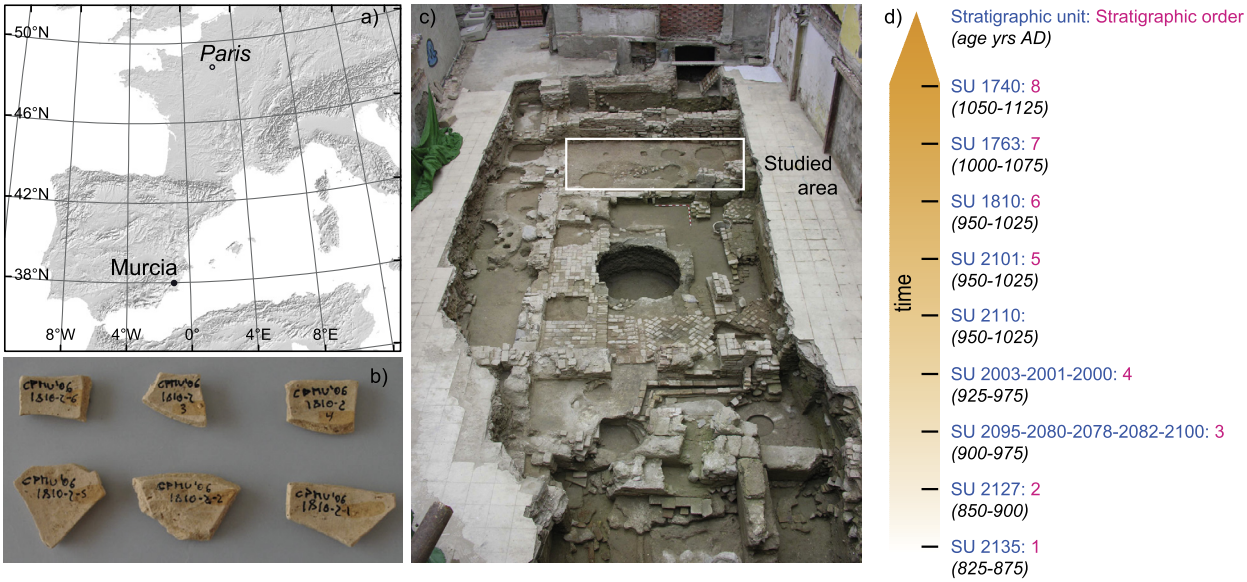

Fig. 1. (a) Location of the archeological site where the archeomagnetic material was recovered (Murcia). The reference location (Paris) where the archeointensity data have been relocated is also shown; (b) picture of the six pottery fragments studied corresponding to the stratigraphic unit SU 1810; (c) photograph of the excavated area (white rectangle); (d) schematic picture showing the temporal sequence of the different stratigraphic units studied. Red numbers correspond to the red circles plotted in Fig. 4. (For interpretation of the references to color in this figure legend, the reader is referred to the web version of this article.)

80 yr). In addition, reconstructions of past solar modulations are crucially dependent on magnetic field strength (Muscheler et al., 2005). This factor and its uncertainties need to be carefully included in the reconstruction of solar activity. In this context, one of the biggest challenges currently facing the paleomagnetic community is to characterize these rapid geomagnetic field intensity events in order to investigate their spatial and temporal variability. Due to the limited number of high-quality intensity data a proper description of geomagnetic field strength during the last millennia is still lacking even for Western Europe, the best-covered region in terms of high-quality archeointensity data. One of the main difficulties in obtaining geomagnetic field reconstructions with a decadal and centennial time scale resolution is the scarcity of precisely dated heated archeological materials. Age uncertainty is perhaps the biggest concern and the most difficult to avoid. Pottery fragments from superimposed strata covering long sequences of occupation provide a powerful tool to recover a clear temporal sequence of the geomagnetic field intensity trend in the past.

In this paper, we report the archeomagnetic study of 79 ceramic fragments collected in the city of Murcia (Southeastern Spain) and that were found in 14 stratigraphic units grouped in 9 consecutive stratigraphic levels (Fig. 1). The present study uses the new data obtained for 8 of the 9 studied levels together with selected high-quality data to investigate the maximum rate of variation of the geomagnetic field strength observed in Western Europe during the last two millennia. Additionally, the spatial and temporal variability and the dipolar/non-dipolar origin of the most significant rapid event (here and after called the 800 AD event) are also investigated by comparing the obtained regional geomagnetic intensity trend with other regional reconstructions and global geomagnetic field models predictions.

2. Archeological context, dating and magnetic characterization

The ceramics studied here were collected in 14 stratigraphic units (SU) identified in a surface no bigger than 3×7 m^2 (white square in Fig. 1c) located in the hearth of the ancient medieval *madîna* of Murcia and corresponding to the long-lasting *andalusí* period. Between four and eight pottery shards per SU were selected for analysis. These SU's are grouped in six consecutive archaeological phases, from phase I (the older phase) to phase VI (the younger phase), and with ages ranging between the 9th and the 12th centuries AD (Fig. 1d). The different phases are defined by different historic moments and can include several SUs. For example, they can be defined by the building of a room and include several SU such as the digging of the foundation ditches, their filling up, the soil that supports pavements, etc. (see Supplementary Material for further details). Several fragments per stratigraphic unit were subjected to rock magnetic analysis in order to gain information about the main magnetic carriers contained in the studied samples. Together (Fig. 2, Supplementary Material), the results indicate that the magnetic mineralogy is dominated by low coercivity phases corresponding to Curie temperatures in the range of 350–590 °C. This suggests that the main magnetic careers are minerals of the titanomagnetite family with very variable Ti contents. In some samples, the presence of a magnetic phase characterized by higher coercivity, Curie and blocking temperatures above 590 °C has also been detected but its remanence contribution is negligible in comparison to the magnetic phase described previously.

3. Paleointensity determination: laboratory protocol

We applied one of the most reliable and widely used approaches for paleointensity determination: the classical Thellier and Thellier method (Thellier and Thellier, 1959) including regular partial thermoremanent magnetization (pTRM) checks and TRM anisotropy and cooling rate corrections. Several pottery fragments per SU and between two and four specimens per fragment were studied. In order to obtain standard paleomagnetic samples, 1 cm $\times$ 1 cm specimens were cut and packed into salt pellets or into quartz cylinders. The archeointensity experiments were conducted at the Paleomagnetic Laboratories of the Institute of Earth Sciences Jaume Almera ICTJA CSIC-CCiTUB (Barcelona, Spain) and Géosciences-Rennes (Rennes, France). Remanent magnetizations were measured using a SRM755R (2G Enterprises) three-axes cryogenic superconducting and Agico JR6 magnetometers. Experiments were made in air and laboratory fields of 50 or 60 μT were applied. Nine to fifteen temperature steps during Thellier experiments were performed between 100 °C and 600 °C. At each

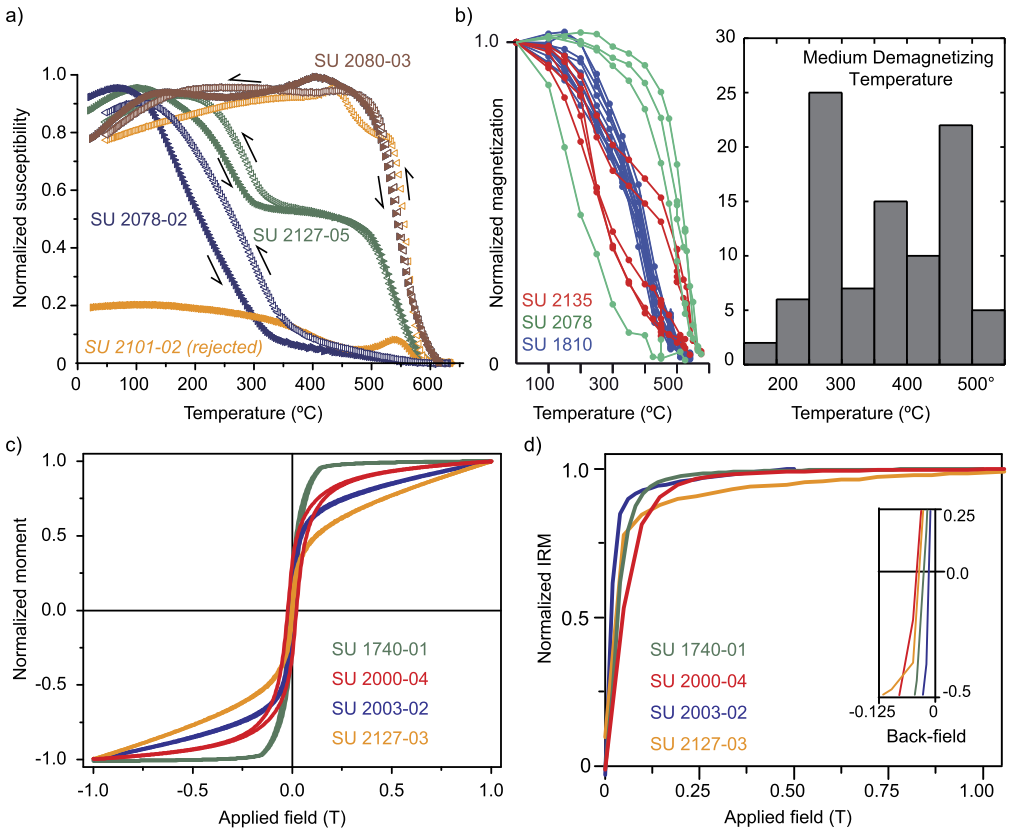

Fig. 2. Rock magnetic properties from representative ceramic fragments. (a–b) Normalized magnetization versus temperature curves and medium demagnetization temperature (MDT), (c) hysteresis loops and (d) normalized IRM acquisition curves and back-field plots. Dark (light) symbols on the thermomagnetic curves indicate the heating (cooling) branches.

Table 1
New archeointensities. Stratigraphic unit and phase; name of the stratigraphic unit and archeological phase where the material was recovered; Stratigraphic order, stratigraphic order of each stratigraphic unit or groups of stratigraphic units (numbers correspond to the red labels in Figs. 1 and 4); Age (yrs AD), assigned age of each stratigraphic unit; *N*, number of independent fragments retained per stratigraphic unit; *n*, number of specimens retained per stratigraphic unit; F ± sd, mean weighted intensity and standard deviation before TRM anisotropy and cooling rate corrections; Fm ± sd, mean weighted intensity and standard deviation corrected for TRM anisotropy; Fpa, mean intensity relocated to Paris; VADM, values of the virtual axial dipole moment. It is worth to notice that the cooling rate effect upon TRM acquisition has been estimated at specimen level (see Table S1) and considered as negligible for this collection.

Stratigraphic unit	Phase	Stratigraphic order	Age (yrs AD)	*N*	*n*	F ± sd (μT)	Fm ± sd (μT)	Fpa (μT)	VADM (10^{22} A m^2)
SU 2135	I	1	[825, 875]	3	5	64.4 ± 3.9	63.1 ± 6.5	71.0	11.2
SU 2127	II	2	[850, 900]	4	6	62.0 ± 6.0	62.9 ± 5.6	70.7	11.1
SU 2095	*III*		*[900, 975]*	*6*	*7*	*69.3 ± 7.5*	*65.1 ± 4.0*		
SU 2080	*III*		*[900, 975]*	*3*	*6*	*57.4 ± 10.3*	*58.5 ± 5.0*		
SU 2078	*III*		*[900, 975]*	*3*	*4*	*69.8 ± 15.2*	*62.9 ± 6.7*		
Mean 2095 + 2080 + 2078	III	3	[900, 975]	12	17	65.5 ± 7.0	62.2 ± 3.4	69.9	11.0
SU 2000	IV	4	[925, 975]	3	4	67.8 ± 3.4	65.6 ± 3.5	73.8	11.6
SU 2101[a]	V	5	[950, 1025]	3	7	61.7 ± 5.5	57.2 ± 5.7	64.3	10.1
SU 1810	V	6	[950, 1025]	6	12	60.3 ± 3.9	57.0 ± 1.8	64.1	10.1
SU 1763	VI	7	[1000, 1075]	4	7	50.1 ± 1.8	46.3 ± 2.2	52.1	8.2
SU 1740[a]	VI	8	[1050, 1125]	4	6	54.6 ± 2.8	52.4 ± 2.5	58.9	9.3

[a] Note that for calculation of these two SU means two anomalous fragments were rejected (see text for further details).

temperature step, samples were first heated and cooled with the laboratory field applied along their *Z*-axis and second, were heated and cooled with the laboratory field applied in the opposite sense. The TRM anisotropy and cooling rate effects upon intensity estimates were determined at the specimen level (see Supplementary Material for further details).

Additionally, strict selection criteria were applied to check the reliability of the intensities determined at the specimen level. pTRM checks have been considered positive if, at a given temperature step, the difference between the original pTRM and the pTRM check does not exceed 10% of the total TRM acquired. We fixed a limit of 50% for the fraction of the initial natural remanent magnetization (NRM) involved for archeointensity determinations (*f* parameter; Coe et al., 1978). Only linear NRM–TRM diagrams corresponding to well defined straight lines going to the origin in the Zijderveld diagrams have been considered. The maximum angular deviation (MAD; Kirschvink, 1980) and the deviation angle (DANG; Pick and Tauxe, 1993) were both restricted to a maximum value of 5°. Finally, mean intensities at the SU level were only retained if were derived from at least two independent fragments (indicated by *N* in Table 1) and four intensity values at the specimen level (indicated by *n* in Table 1). The protocol applied

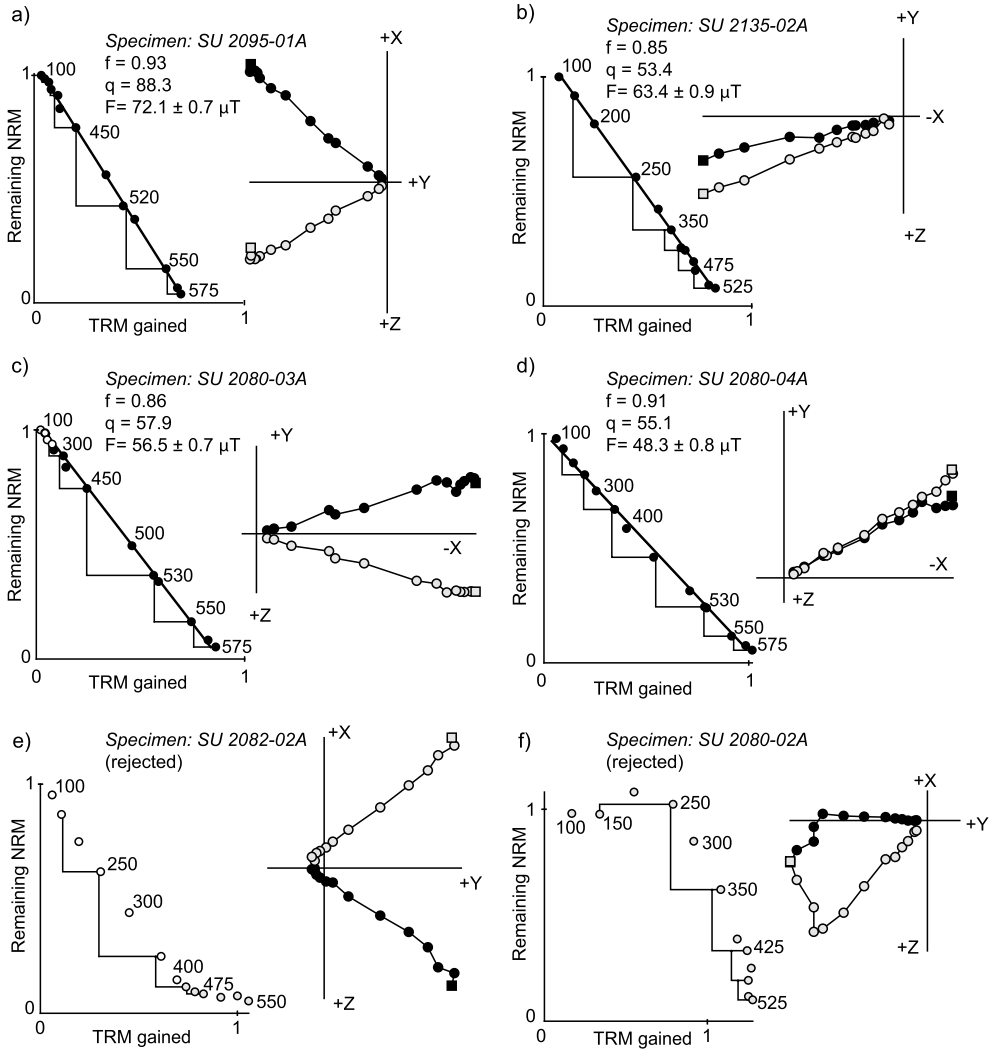

Fig. 3. Thellier archeointensity results. Typical NRM–TRM diagrams. Examples of accepted (a–d) and rejected (e–f) archeointensity results of representative specimens. The NRM–TRM diagrams are shown together with the Zijderveld diagrams, in sample coordinates. In the Zijderveld diagrams open (solid) circles are projections upon vertical (horizontal) planes. NRM/TRM plots are normalized to the initial NRM intensity and closed circles correspond to data used for archeointensity determinations. The archeointensity (F) without TRM anisotropy correction, the NRM fraction used for calculation of the paleointensity (f) and the quality factor (Coe et al., 1978) are also indicated.

provides, in our opinion, the bases to recover highly reliable estimates of past field intensity.

4. Results: new archeointensity data for Western Europe

Thellier experiments were attempted on 79 pottery fragments. Two types of behavior have been observed. In some cases well-defined straight lines going toward the origin after removal of a weak secondary component of magnetization during the first temperature steps are observed (Fig. 3a–d). This (characteristic) component likely corresponds to the TRM acquired during the manufacture of the pottery fragments. The maximum unblocking temperatures observed range between ~320–350 °C and 580 °C, which is in agreement with the rock-magnetic results described in Section 3. For these specimens linear NRM–TRM diagrams have been obtained. In other samples, we observed a complex behavior, with straight lines not going toward the origin (Fig. 3e) or with two clear components of magnetization in the Zijderveld diagrams (Fig. 3f). In order to only consider the most reliable archeointensities we discarded the estimations based on this type of behavior. 74 archeointensities satisfied the selection criteria applied at the specimen level. Mean intensities at the SU level were only retained if derived from at least four specimens. This cut-off number of specimens corresponds to the A and B "high-quality" categories defined in Pavón-Carrasco et al. (2014a). This results in a total of 67 accepted intensity values, corresponding to 41 different fragments (Supplementary Table S2). The NRM fraction used for archeointensity determination ranges between 0.51 and 0.93 and the quality factors q between 4.7 and 88.3. Specimens 2135-03B, and 1740-06B corresponding to MAD = 5.6° and MAD = 5.1°, respectively, were accepted as they meet all the other quality standards described before in Section 4 and sister specimens provide very similar intensities (Supplementary Table S2). Approximately 50% of the studied fragments were rejected for archeointensity determination. This success rate is low in comparison with archeointensity studies performed on repeatedly heated structures for which a more stable rock-magnetic behavior is generally observed (e.g. Gómez-Paccard et al., 2006, 2012b; Catanzariti et al., 2012) but similar to paleointensity experiments performed on ceramic fragments (e.g. Tema et al., 2012; Genevey et al., 2013).

As expected, differences between uncorrected and TRM anisotropy corrected values at the specimen level are high (more than 10%) for some of the specimens. It is worth noting that very different TRM anisotropy correction factors can be obtained for spec-

imens from the same fragment. For example, the TRM correction factor is −4.8% for the specimen 2135-03A and 11.7% for specimen 2135-03B. This confirms that this effect should be studied and corrected separately for each specimen when studying pottery fragments for archeointensity determination. For the specimens prepared using salt pellets no control of the exact position of the specimens was possible. In contrast, the quartz cylinders technique allowed controlling the relative position of sister specimens during heating. When feasible and for sister specimens, the magnetic field was applied in two perpendicular directions (for one specimen perpendicular to the fragment surface, i.e., along the difficult axis of magnetization, and for the other parallel to it, i.e., along the easy axis). This orientation control allowed additional testing of the TRM anisotropy correction applied. For example specimens 2080-01A and 2080-01D, both of them from the same fragment, yielded archeointensities of 75.7 ± 2.3 and 65.9 ± 1.8 μT, respectively, before TRM anisotropy correction (Table S2). The laboratory field was applied perpendicular to the fragment surface in specimen 01-A, whereas it was approximately parallel in 01-B. It is noticeable how archeointensities after TRM correction only differed in 2.3 μT (65.8 ± 2.1 and 63.5 ± 1.6 μT). This value is within the statistical level of uncertainty. This test confirms the good performance of the applied TRM anisotropy corrections. For ∼50% of the studied specimens the magnetic alteration during the cooling rate protocol hampered a reliable estimation of the cooling rate factor (see Table S2). For the other specimens, the results indicate that the cooling rate effect upon TRM acquisition is low (<5%), being the mean value of about 1.9% (see Table S2). Therefore, the cooling rate effect upon TRM acquisition has been considered as negligible for the overall collection and no cooling rate correction factors were applied.

In general, specimens from the same fragment give very similar TRM corrected intensities (see for example SU 2135-01A and -01B or SU 2080-04A and -04C). But some important differences are observed for other fragments (SU 2127-04A and -04B), highlighting the appropriateness of measuring several fragments per SU and several specimens per fragment. From the TRM corrected archeointensities obtained at the specimen level (Table S2) we calculate mean fragment values. The fragment means were then used to derive the mean intensities at the SU level, derived using the mean weighting factors defined by Prévot et al. (1985).

Three "anomalous" high intensities are obtained for SU 2101-03A, SU 1740-05A and SU 1740-05B (marked with stars in Table S2) in comparison with the other results obtained for the SU concerned (in particular seven specimens for SU 2101 and six for SU 1740). The rejection of these "anomalous" specimens led to a sharp decrease in the standard deviation (sd) of the means at the SU level. For example, if the specimen SU 2101-03A is retained a very high sd around the mean is obtained (66.5 ± 13.4 μT, ∼20%). This high sd is due to the SU 2101-03A intensity value (83.2 ± 1.0 μT after the TRM anisotropy correction) that gives an anomalously high intensity, but very well defined, in comparison with the other seven specimens of the same site which led to a much lower intensity range between 51.0 and 66.3 μT. We can, therefore, reasonably suspect that some problems occurred during the selection of the pottery fragments at the archeological site or that this anomalous fragment corresponds to a different age interval than the other fragments of SU 2101. If this "outlier" data is rejected the SU 2101 mean is 61.7 ± 5.5 μT before TRM anisotropy correction and 57.2 ± 5.7 μT, after TRM anisotropy correction. A similar phenomenon is observed for specimens SU 1740-5A and -5B. We, therefore, reject these three specimens for further interpretation (however the "anomalous" intensity values at the specimen level are also included in Table S2).

The ten SU mean intensities are summarized in Table 1. They have been obtained and derived from at least 3 independent pottery fragments and 4 specimens. The standard deviations of the SU means are lower than 6.7 μT (or ∼10% of the means). Considering the archeological and stratigraphic constraints described in section 2, we calculate a mean intensity for the period 900–975 AD using SU 2095, SU 2080 and SU 2078 that correspond to the same stratigraphic level and age interval (Fig. 1d). Therefore, height new high-quality mean intensities have been obtained. The final intensities proposed are listed in Table 1 where the relative stratigraphic order is also indicated (numbers from 1 to 8 in Table 1 and Fig. 1d, Fig. 4 red circles). The new data provide a temporal sequence of past intensity changes in Southeastern Spain between the 9th and the 12th centuries AD. Intensity values between 73.8 ± 3.5 μT (11.6×10^{22} A m^2, SU 2000) and 52.1 ± 2.2 μT (8.2×10^{22} A m^2, SU 1763) were obtained.

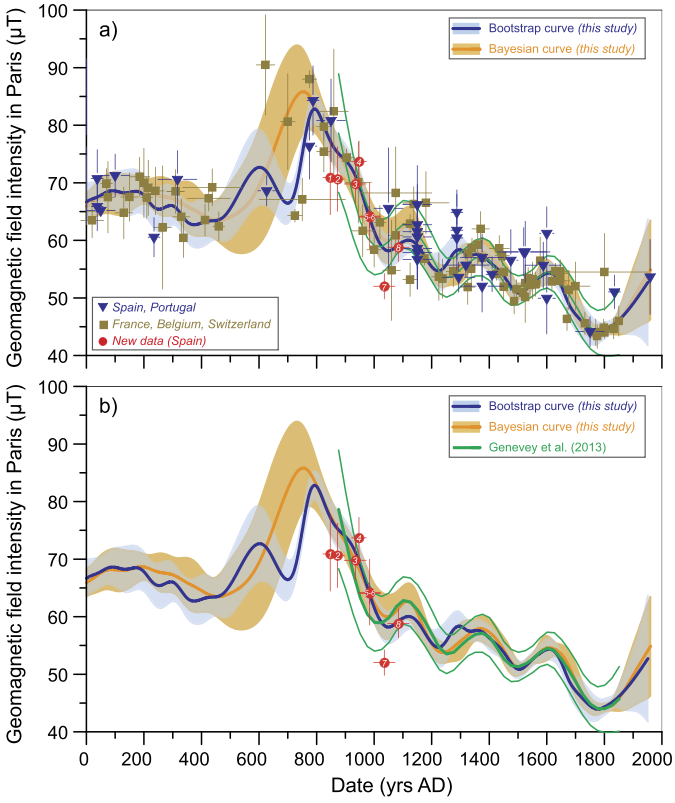

Fig. 4. Past geomagnetic field intensity changes in Western Europe. (a) New archeointensity data obtained in this study (red circles) together with selected high-quality results (see text for explanation of the selection criteria used). Archeointensity data are all referred to Paris (France). Red numbers indicate the temporal (stratigraphic) sequence of the different levels studied. These temporal constraints provide an additional tool to interpret geomagnetic field intensity past changes. The mean Bayesian and Bootstrap curves derived from the selected data are shown in orange and blue, respectively, together with their 95% envelopes (orange and blue areas). (b) The new data and curves obtained in this study compared with the intensity curve of Genevey et al. (2013). (For interpretation of the references to color in this figure legend, the reader is referred to the web version of this article.)

Considering the new data obtained and the chronological and stratigraphic constraints described previously (Fig. 1d), an intensity decrease of 19.3 μT between 950 AD (SU 2000, point 4 in Fig. 4 and Table 1) and 1040 AD (SU 1763, point 7) is deduced if the mean age and mean intensity value are considered. This corresponds to a rapid change of the geomagnetic field strength in the area of about 22 μT/century. The new data also suggest that a rapid intensity increase of about 6 μT occurred during the 11th century in Murcia. A relative minimum value is obtained for SU 1763 (point 7, 46.3 ± 2.2 μT, 1037.5 AD) followed by a rapid intensity increase (SU 1740, point 8, 52.4 ± 2.5 μT, 1087.5 AD). We would like to point out, however, that these rates of changes they

are rough estimates and more sophisticated analysis and additional data are required to probe more deeply into the details of geomagnetic field behavior during these rapid events.

5. Discussion: the 800-AD European event: a regional or a global signature?

As mentioned above, several recent studies have attempted to constrain the spatio-temporal characteristics of different regional rapid intensity events (e.g., Ben-Yosef et al., 2009; Ertepinar et al., 2012; Shaar et al., 2011, 2015; Gallet et al., 2015). Extreme geomagnetic field intensity changes in the range of 400–500 μT/century ca. 1000 BC in the Near East have been proposed (Ben-Yosef et al., 2009; Shaar et al., 2011). These extreme values, not observed elsewhere at the Earth's surface, are not compatible with our current understanding of the Earth's dynamo (Livermore et al., 2014). Europe, the best-covered region in terms of high-quality archeomagnetic intensity data (Pavón-Carrasco et al., 2014a), offers a unique opportunity to obtain a detailed description of past geomagnetic field intensity changes at decadal-centennial time scales, a resolution currently hard-to-access in other regions. Our current knowledge demonstrate that several rapid intensity fluctuations related to rates of change of at least 5–10 μT/century occurred in Western Europe over the last 2 ka (Genevey et al., 2009, 2013; Gómez-Paccard et al., 2008, 2012a). However, these rates are determined from averaged local curves and the existence of episodes with larger intensity variations rates cannot be excluded. These studies clearly evidence that the most important intensity feature observed for the last 2 ka is the high intensity feature first identified in France by Genevey and Gallet (2002) and related to a strong intensity decrease between the first half of the 9th century and the 12th century. Recently, Gómez-Paccard et al. (2012a) indicate that the 800 AD event took place at the continental European scale and was probably related to a double oscillation of the field intensity with the maximum values occurring around 600 and 800 AD. This double oscillation is well defined for Eastern Europe but still requires confirmation in the western part of this region. The new data obtained here focuses on the decreasing part of this intensity feature. The obtained intensities were relocated to Paris (latitude 48.9°N, longitude 2.3°E) by the Virtual Axial Dipole Moment method and are plotted in Fig. 4. The new data provide an improved description of the 800 AD event and help to better define the intensity minimum that took place around 1050 AD.

In order to obtain an up-to-date reconstruction of geomagnetic field strength fluctuations in Western Europe, we selected high-quality archeointensities for the last 2250 years. This selection corresponds to the A and B quality categories previously defined in Pavón-Carrasco et al. (2014a), i.e. data derived from at least 4 specimens and obtained from the original or derived Thellier and Thellier method including pTRM checks and TRM correction via TRM anisotropy tensor whatever the material analyzed is, or data not including the TRM anisotropy correction but obtained from unlikely anisotropic objects (e.g. kilns, hearths, burnt soils). Data determined by the Triaxe vibrating sample magnetometer protocol (Le Goff and Gallet, 2004) and derived from at least 4 specimens are also included in these categories. A total of 135 data from France (91), Spain (34), Portugal (2), Switzerland (5), and Belgium (3) fulfills these eligibility criteria. Two mathematical approaches have been applied to the selected dataset. First, we used the Bayesian approach based on roughness penalty (Lanos, 2004). This approach uses variable window widths that are automatically adapted to the density of points along the time axis. The advantages of this method include that it naturally takes into account the intensity and dating errors and assumptions concerning what is physically reasonable are encoded through prior probability density functions. The stratigraphic constraints available for the archeological materials are also considered (for example for the potteries studied here, numbers from 1 to 8, Fig. 4a). And second, we used the iteratively reweighted least-squares algorithm combined with a Bootstrap approach following Thébault and Gallet (2010), which also explores the effect of dating and intensity errors on the master curve estimation. The Bootstrap and Bayesian results are plotted in Fig. 4a (see also Supplementary Tables S3 and S4) as a mean curve (orange and blue dark lines, respectively) together with their error at 95% confidence (orange and blue shaded bands). The two obtained master curves are very similar for the periods with a high density of data, that is 0–450 AD and 800–1900 AD, showing small intensity fluctuations during the first above-mentioned period with a relative maximum around 200 AD and a relative minimum around 350–450 AD. Between 800 and 1900 AD, three short intensity peaks, similar to those observed by Genevey et al. (2013), are identified in both curves (Fig. 4b). However, some differences are observed between 450 and 800 AD. While the Bayesian curve is characterized by a maximum value of the intensity of about 85.9 μT at 750 AD, the Bootstrap curve gives some support to the presence of a double intensity oscillation with the two maxima achieved at 600 AD (72.8 μT) and 800 AD (82.8 μT). The differences between both estimates are clearly due to the scarcity of data and, therefore, the master curves obtained here for this period must be considered with caution. It would be worthwhile to obtain new data for the interval 450–800 AD to resolve the single or double character of this event. Whatever the case, from 800 AD to around 1050 AD, both curves show a well defined intensity decay (Fig. 4b).

From the Bayesian and Bootstrap master curves, the rate of intensity change can be calculated. Recourse to determining an average rate of change over the most significant increasing or decreasing trends is unfortunately all that appears possible given the presently available dataset and curves. The rates of change calculated here are, obviously, a simplification of the true evolution of the geomagnetic field. They should be interpreted as the average rate of change for the periods defined in Table 2, rather than constant rates of change for the entire interval. Rapid fluctuations corresponding to shorter time scales cannot be excluded considering our current archeointensity dataset (see for example differences between our new data 5–6, 7 and 8, red circles in Fig. 4). The mean rates obtained (Table 2) confirm that several rapid intensity changes took place in Western Europe over the last 2 ka. Excluding the 500–800 AD period for which the curves are not well constrained, rates of change of about 7–10 μT/century are observed between 800 and 1000 AD, between 1100 and 1225 AD and for 1600–1780 AD. Curiously the maximum rates are related with the decrease of the geomagnetic field strength. Interspersed

Table 2
Averaged intensity ratios (μT/century) for the time intervals shown in the first column.

Time interval (AD)	Bayesian (this study)	Bootstrap (this study)
0–500	−0.9	−1.2
500–800	*10.1*	*7.6/−7.6/18.0*[a]
800–1000	−9.9	−9.5
1000–1100	4.5	3.0
1100–1225	−9.5	−6.2
1225–1350	3.6	2.3
1350–1500	−5.4	−5.1
1500–1600	4.3	4.0
1600–1780	−7.5	−7.0
1780–1900	5.0	4.3

[a] The bootstrap curve presents in this period a minimum around 700 AD, for this reason we provided 3 different intensity rates corresponding to increasing/decreasing parts of the curve. We remind here that for the interval 500–800 AD the results must be interpreted with caution.

pulses of partial paleointensity recovery occurred, but rarely exceed rates of 4 μT/century. These high rates of about 10 μT/century are perfectly compatible with the predicted rates of change per century in total intensity at the Earth's surface for the interval 2015–2020 as predicted by the 12th generation of the IGRF model (Thébault et al., 2015) for other mid latitudes locations. For example, for the 2015–2020 time interval, the IGRF-12 (Thébault et al., 2015) predicts the largest decreasing rate in intensity to take place in the center of North America (with rates of 11–12 μT/century) as well as the South-eastern Pacific Ocean (10 μT/century) whereas the largest increasing rate (of about 10 μT/century) is predicted at the Southern Indian Ocean. For a longer interval, the IGRF-12 model also indicates an almost linear decrease in intensity since 1940 until the present for the SSA, with an average decrease of 3.4 μT/century. Our data therefore demonstrates that similar (and higher) rates of intensity decrease have been often seen over the past 2 millennia. The rates of change obtained for the last 2000 years in Western Europe are also compatible with the upper limit of 62 μT/century (at the Earth's surface) proposed by Livermore et al. (2014) from numerical simulations of the Earth's geodynamo.

Another major – and difficult – issue taking into account the state-of-the-art of the current archeointensity global dataset concerns the evaluation of the origin and nature of the observed rapid geomagnetic field intensity variations (e.g., Gallet et al., 2003, 2009; Knudsen et al., 2008; de Groot et al., 2013; Mitra et al., 2013). These events might have a regional or a global character depending on their dominant non-dipolar or dipolar harmonic sources, respectively. To investigate this, we first compared the local VADM estimations for Western Europe (from this study), Bulgaria (Kovacheva et al., 2014) and the Middle East (Gallet et al., 2015) directly computed from the corresponding regional intensity curves (Fig. 5a). The VADM values are the equivalent axial dipole moments that would produce the observed intensity at these latitudes. Obviously, any non-dipole field contribution will distort individual VADM result compared to the true axial dipole moment (ADM). This comparison shows that high VADM values (of more than $12 \cdot 10^{22}$ A m^2) were achieved in the European continent between 500 and 1000 AD: maximum values are observed both in Western Europe and in Bulgaria (Eastern Europe). The results indicate the non-synchronization of the VADM maxima from Western (∼790 AD in Paris) and Eastern (∼933 AD in Sofia) Europe suggesting an eastward drift of the geomagnetic field in the European region. However, in the Middle East curve (Gallet et al., 2015) this maximum is not clearly observed. This is probably due to the high dispersion of the data that produces a smoother trend. If we apply the three selection criteria described before to the Middle East intensity data corresponding to a 1000-km radius circle around the location (36° 49′N and 40° 02′E, the same region used in Gallet et al., 2015) only six high-quality data are available (see Supplementary Material Figure S2). Therefore, and taking into account the available data it is not clear if the studied geomagnetic field intensity feature dissipates eastwards or not.

In order to estimate the origin of the 800 AD event in terms of dipolar or non-dipolar sources, we compared it with the dipole moment estimations at global scales. In this sense, some previous considerations must be highlighted. Averaging of globally distributed VADMs or VDMs can mitigate the dipole moment distortion related to non-dipolar sources. However, care has to be taken with inhomogeneous data distributions and as it has been recently showed that global modeling approach provides more reliable estimations of the geomagnetic dipole moment than averaged weighting approaches even if strongly biased databases are used (Campuzano et al., 2015). In Fig. 5b we plot global averaged VADM/VDM reconstructions constructed by applying temporal and geographical averages to all the available data

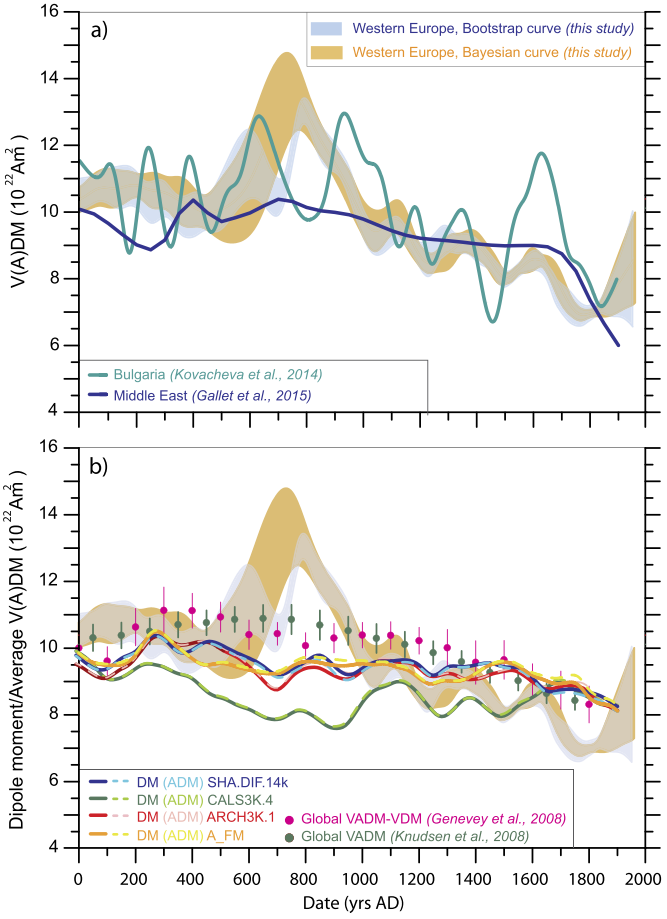

Fig. 5. Comparison between the geomagnetic field intensity (transformed into VADM) variation curves in Western Europe (this study, in orange and blue shaded area) with a) the VADM regional curves from Bulgaria (Kovacheva et al., 2014), the Middle East (Gallet et al., 2015) and b) global VADM and mixed VADM–VDM estimations (Genevey et al., 2008; Knudsen et al., 2008); and dipole moment (DM) and axial dipole moment (ADM) estimation derived from the time-dependent spherical harmonic global models of the Earth's magnetic field ARCH3K.1 (Korte et al., 2009), CALS3K.4 (Korte and Constable, 2011), A_FM (Licht et al., 2013) and SHA.DIF.14k (Pavón-Carrasco et al., 2014b). (For interpretation of the references to color in this figure legend, the reader is referred to the web version of this article.)

(Knudsen et al., 2008) and to selected data fulfilling certain quality criteria (Genevey et al., 2008). They are seen to be more or less constant during the first millennium AD (oscillating between 9.5 and $11 \cdot 10^{22}$ A m^2) and to have decreased up to $\sim 8.5 \cdot 10^{22}$ A m^2 at 1800 AD. We thus also compute the dipole moment (DM, calculated from the three first Gauss coefficients) and the axial dipole moment (ADM, calculated from g_1^0) derived from the most recent spherical harmonic (SH) global models based on paleo/archeomagnetic data. The time-varying Gauss coefficients derived from the ARCH3k.1 (Korte et al., 2009), the CALS3k.4 (Korte and Constable, 2011), the A_FM (Licht et al., 2013) and the SHA.DIF.14k (Pavón-Carrasco et al., 2014b) global models were used to estimate the fluctuations of the DM and ADM over the past 2 ka (Fig. 5b). It is interesting to note that the VADM/VDMs global estimates are systematically higher than the geomagnetic dipole moment based on spherical harmonic analysis for the 0–1300 AD interval. The data quality, the effect of uncorrected averaged non-dipolar contributions, and the fact that the available data distribution is extremely biased towards the Northern hemisphere are the responsible for the discrepancy between global averaged V(A)DM and (A)DM (see Campuzano et al., 2015 for more details).

All the different geomagnetic field models with the exception of the CALS3K.4 show the same general (A)DM behavior. The

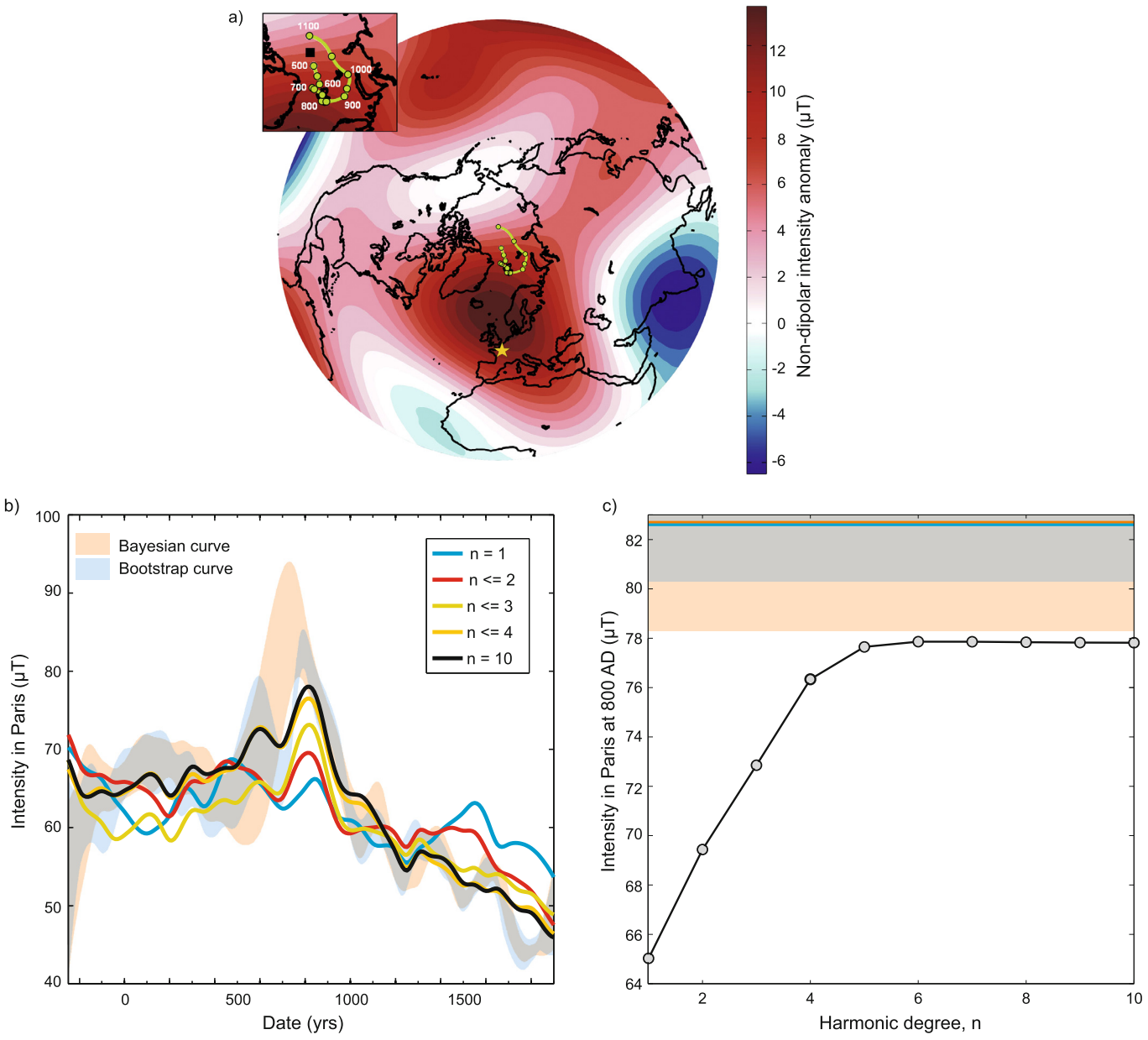

Fig. 6. a) Map of the North Hemisphere showing the differences between the total intensity and the dipolar intensity at 800 AD as predicted by the SHA.DIF.14k model (Pavón-Carrasco et al., 2014b). The green curve represents the predicted positions of the North geomagnetic pole (from 500 AD up to 1100 AD) and the yellow star the location of Paris. b) Intensity curve in Paris using different harmonic contributions from 250 BC to 1900 AD. c) The intensity at 800 AD in Paris as a function of the harmonic degree n (considering all the order m, i.e. $m = 0, 1 \ldots n$). The intensity values were synthesized using the global model SHA.DIF.14k. In b) and c) the mean Bayesian and Bootstrap curves obtained in this study are shown in orange and blue, respectively, together with their 95% envelopes (orange and blue areas). (For interpretation of the references to color in this figure legend, the reader is referred to the web version of this article.)

CALS3K.4 model gives significantly low dipole moment estimations before 1650 AD that could be attributed to the re-calibration of the sediment records used in the modeling approach (Korte and Constable, 2011). We therefore exclude this model for the following discussion and only use the models exclusively based on archeomagnetic and lava flow data.

We find that the dipole moment has been continuously decreasing since 250 AD, with values ranging between 10.3 and $8.3 \cdot 10^{22}$ A m^2, approximately. The (A)DM trends show several small short-term oscillations superimposed to this general behavior. Some of these small fluctuations are different for the three models due to the different model parameters used for their construction since the databases were similar. It can be seen that they all show a relative maximum around 850 AD (of about $9.8 \cdot 10^{22}$ A m^2) achieved after a partial recovery from a minimum at 700 AD ($9.2 \cdot 10^{22}$ A m^2), approximately. A relative minimum of about $9.5 \cdot 10^{22}$ A m^2 is also predicted at 950 AD. Although being subject to some uncertainties – as evidenced by the differences between the results computed from the different global models – the larger discrepancies between the (A)DM estimates and the regional VADM curves for Western Europe are clearly observed for the 500–1000 AD period. This may suggests a significant non-dipolar contribution to the high-intensity 800 AD event. It is noticeable that the small (A)DM fluctuation around 850 AD presents similar values of magnitude than other variations for the last 2 ka (Fig. 5b), and it seems that none of them are linked to pronounced high-intensity events.

In order to obtain the non-dipolar contribution from the global geomagnetic field models we subtracted the dipole field (i.e. the first 3 Gauss coefficients) to the total field. We thus compared

the paleosecular variation curves in Paris directly computed from archeomagnetic data with the predictions in Paris given by three different models (Supplementary Figure S3). None of the models reported here capture a significant maximum in the dipolar intensity for the 500–1000 AD interval. Only two small relative maxima around 500 and 850 AD are observed.

To analyze the possible effect of the tilt of the dipole axis towards Western Europe, we have also computed the polar path of the geomagnetic pole predicted by the SHA.DIF.14k model (Fig. 6a). We use this model since it is the global model that better fit the 800 AD event (Supplementary Material). It can be seen how, in fact, the pole moves towards Western Europe between 500 and 800 AD. This movement should induce simultaneous enhancements of the intensity and inclination in Paris, as it is already seen in Figs. S3c and S3e. In order to go deep in this issue, we have quantified the difference in the intensity produced by an axial dipole ($n = 1$, $m = 0$) and by a tilted dipole ($n = 1$, $m = 0$, 1) at 800 AD. A value of 5 μT is obtained from the SHA.DIF.14k. This suggests that a tilted dipole cannot totally explain the high intensity increase observed in Paris around this period.

The observations above mentioned indicate that, on the basis of the current state of geomagnetic field global models, non-dipolar terms must be considered to predict the 800 AD event in Europe. We therefore sought to quantify the contribution of the different harmonic terms to the intensity curve predicted in Paris (Fig. 6b). The results show how different intensity patterns are predicted depending on the used harmonic degree n. For the 800 AD event, we can see how this maximum increases as higher degree harmonics are considered: an intensity value of 65.0 μT is predicted for $n = 1$, which rapidly increases to 69.4, 72.9 and 76.3 μT and 77.6 for $n = 2$, 3, 4 and 5, respectively. For $n \geq 6$ an intensity of about 78 μT is obtained (Fig. 6c). The largest harmonic contributions are given by the quadrupole (degree $n = 2$), octupole (degree $n = 3$), and 4-multipole (degree $n = 4$) terms (Fig. 6c).

Finally, we investigate the spatial variation of this geomagnetic field intensity feature and plotted the differences between the total intensity field and the intensity dipolar field at 800 AD for the whole North hemisphere (Fig. 6a). The map shows a clear intensity anomaly of non-dipolar origin that covers North-Central Europe with a maximum of around 13 μT centered in the Norwegian Sea, just to the north of the United Kingdom. This positive intensity anomaly is the main responsible of the maximum observed in Paris at 800 AD. The extension of this anomaly (about $11 \cdot 10^3$ km from South to North and $7 \cdot 10^3$ from East to West) agrees, in average, with the spatial half-wavelength characteristic of the quadrupolar, octupolar and 4-multipolar fields, i.e. around $10 \cdot 10^3$, $6.5 \cdot 10^3$ and $5 \cdot 10^3$ km, respectively.

6. Conclusion

Eight new highly reliable intensity data have been obtained for Western Europe from the study of well-dated pottery fragments. The new data provide a better description of the 800 AD event, the most important change observed in Europe during the last 2000 years. The results derived from global modeling suggest that this event is linked to a large non-dipolar source of the geomagnetic field, at that time centered in the Norwegian Sea. This anomaly probably induced the rapid high-intensity events observed at the European continent (from Paris to Sofia) over the 500–1000 AD period. It is important to notice that current global geomagnetic field models are nowadays constructed considering the complete archeomagnetic and/or volcanic databases (no quality selection criteria have been applied to select the most reliable paleointensities). Whatever the predicted results correspond to a real geomagnetic field behavior or not will be confirmed by additional high-quality intensity data and future improved regional and global geomagnetic reconstructions. We acknowledge that new data are essential to gain insight into the spatial and temporal evolution of this and other similar rapid geomagnetic intensity features.

Acknowledgements

Data available upon request to mgomezpaccard@igeo.ucm-csic.es. M.G.P acknowledges the Ramón y Cajal Program and the CGL2015-63888-R research project of the Spanish Ministry of Economy and Competitiveness. Financial support was also given by a sabbatical within the Salvador de Madariaga program (PR20110248, MECD) and by the CGL2014-54112-R research projects from the Spanish Ministry of Education and Science. F.J.P.C. is funded from the European Union's Horizon 2020 research and innovation programme under the Marie Sklodowska-Curie grant agreement No. 659901. We would like to extend our warm thanks to our colleagues of the paleomagnetic laboratories of Barcelona (ICTJA CSIC-CCiTUB), Rennes (Géosciences-Rennes) and Burgos (CENIEH) where the magnetic measurements have been conducted. We thank R. Shaar and an anonymous reviewer for a thorough review of this manuscript.

Appendix A. Supplementary material

Supplementary material related to this article can be found online at http://dx.doi.org/10.1016/j.epsl.2016.08.024.

References

Ben-Yosef, E., Tauxe, L., Levy, T.E., Shaar, R., Ron, H., Najjar, M., 2009. Geomagnetic intensity spike recorded in high resolution slag deposit in southern Jordan. Earth Planet. Sci. Lett. 287, 529–539.

Cai, S., Tauxe, L., Deng, C., Pan, X., Jin, G., Zheng, J., Xie, F., Qin, H., Zhu, R., 2014. Geomagnetic intensity variations for the past 8 kyrs: new archaeointensity results from eastern China. Earth Planet. Sci. Lett. 392, 217–229.

Campuzano, S.A., Pavón-Carrasco, F.J., Osete, M.L., 2015. Non-dipole and regional effects on the geomagnetic dipole moment estimations. Pure Appl. Geophys. 172, 91–107. http://dx.doi.org/10.1007/s00024-014-0919-3.

Catanzariti, G., Gómez-Paccard, M., McIntosh, G., Pavón-Carrasco, F.J., Chauvin, A., Osete, M.L., 2012. New archaeomagnetic data recovered from the study of Roman and Visigothic remains from central Spain (3rd–7th centuries). Geophys. J. Int. 188 (3), 979–993.

Coe, R.S., Grommé, C.S., Mankinen, E.A., 1978. Geomagnetic paleointensities from radiocarbon-dated lava flows on Hawaii and the question of the Pacific nondipole low. J. Geophys. Res. 83, 1740–1756.

de Groot, L.V., Biggin, A.J., Dekkers, M.J., Langereis, C.G., Herrero-Bervera, E., 2013. Rapid regional perturbations to the recent global geomagnetic decay revealed by a new Hawaiian record. Nat. Commun. 4, 2727. http://dx.doi.org/10.1038/ncomms3727.

Ertepinar, P., Langereis, C.G., Biggin, A.J., Frangipane, M., Matney, T., Ökse, T., Engin, A., 2012. Archaeomagnetic study of five mounds from Upper Mesopotamia between 2500 and 700 BCE: further evidence for an extremely strong geomagnetic field ca. 3000 years ago. Earth Planet. Sci. Lett. 357–358, 84–98.

Gallet, Y., Genevey, A., Courtillot, V., 2003. On the possible occurrence of archaeomagnetic jerks in the geomagnetic field over the past three millennia. Earth Planet. Sci. Lett. 214, 237–242.

Gallet, Y., Hulot, G., Chulliat, A., Genevey, A., 2009. Geomagnetic field hemispheric asymmetry and archeomagnetic jerks. Earth Planet. Sci. Lett. 284, 179–186.

Gallet, Y., Molist, M., Genevey, A., Clop, X., Thébault, E., Gómez, A., Le Goff, M., Robert, B., Nachasova, I., 2015. New Late Neolithic (c. 7000–5000 BC) archeointensity data from Syria. Reconstructing 9000 years of archeomagnetic field intensity variations in the Middle East. Phys. Earth Planet. Inter. 238, 89–103.

Genevey, A., Gallet, Y., 2002. Intensity of the geomagnetic field in Western Europe over the past 2000 years: new data from ancient French pottery. J. Geophys. Res. B 11 (107), 2285. http://dx.doi.org/10.1029/2001JB000701.

Genevey, A., Gallet, Y., Constable, C.G., Korte, M., Hulot, G., 2008. ArcheoInt: an upgraded compilation of geomagnetic field intensity data for the past ten millennia and its application to the recovery of the past dipole moment. Geochem. Geophys. Geosyst. 9 (4), Q04038. http://dx.doi.org/10.1029/2007GC001881.

Genevey, A., Gallet, Y., Rosen, J., Le Goff, M., 2009. Evidence for rapid geomagnetic field intensity variations in Western Europe over the past 800 years from new French archeointensity data. Earth Planet. Sci. Lett. 284, 132–143. http://dx.doi.org/10.1016/j.epsl.2009.04.024.

Genevey, A., Gallet, Y., Thébault, E., Jesset, S., Le Goff, M., 2013. Geomagnetic field intensity variations in Western Europe over the past 1100 years. Geochem. Geophys. Geosyst. 14, 2858–2872.

Gómez-Paccard, M., Chauvin, A., Lanos, P., Thiriot, J., Jimenez-Castillo, P., 2006. Archeomagnetic study of seven contemporaneous kilns from Murcia (Spain). Phys. Earth Planet. Inter. 157, 16–32.

Gómez-Paccard, M., Chauvin, A., Lanos, P., Thiriot, J., 2008. New archeointensity data from Spain and the geomagnetic dipole moment in Western Europe over the past 2000 years. J. Geophys. Res. 113 (B9), B09103.

Gómez-Paccard, M., Chauvin, A., Lanos, P., Dufresne, P., Kovachevad, M., Hill, M.J., Beamud, E., Blain, S., Bouvier, A., Guibert, P., Archaeological Working Team, 2012a. Improving our knowledge of rapid geomagnetic field intensity changes observed in Europe between 200 and 1400 AD. Earth Planet. Sci. Lett. 355–356, 131–143.

Gómez-Paccard, M., McIntosh, G., Chauvin, A., Beamud, E., Pavón-Carrasco, F.F., Thiriot, J., 2012b. Archaeomagnetic and rock magnetic study of six kilns from North Africa (Tunisia and Morocco). Geophys. J. Int. 189, 169–186.

Hervé, G., Chauvin, A., Lanos, P., 2013. Geomagnetic field variations in Western Europe from 1500 BC to 200 AD. Part II: new intensity secular variation curve. Phys. Earth Planet. Inter. 218, 51–65.

Hong, H., Yu, Y., Lee, C.H., Kim, R.H., Park, J., Doh, S-J., Kim, W., Sung, H., 2013. Globally strong geomagnetic field intensity circa 3000 years ago. Earth Planet. Sci. Lett. 383, 142–152.

Kirschvink, J.L., 1980. The least-squares line and plane and the analysis of paleomagnetic data. Geophys. J. R. Astron. Soc. 62, 699–718.

Knudsen, M.F., Riisager, P., Donadini, F., Snowball, I., Muscheler, R., Korhonen, K., Pesonen, L.J., 2008. Variations on the geomagnetic dipole moment during the Holocene and the past 50 kyr. Earth Planet. Sci. Lett. 272, 319–329.

Korte, M., Constable, C., 2011. Improving geomagnetic field reconstructions for 0–3 ka. Phys. Earth Planet. Inter. 188, 247–259.

Korte, M., Donadini, F., Constable, C., 2009. Geomagnetic field for 0–3 ka: 2. A new series of time-varying models. Geochem. Geophys. Geosyst. 10, Q06008. http://dx.doi.org/10.1029/2008GC..2297.

Kovacheva, M., Kostadinova-Avramova, M., Jordanova, N., Lanos, P., Boyadzhiev, Y., 2014. Extended and revised archaeomagnetic database and secular variation curves from Bulgaria for the last eight millennia. Phys. Earth Planet. Inter. 236, 79–94.

Lanos, P., 2004. Bayesian inference of calibration curves: application to archaeomagnetism. In: Buck, C., Millard, A. (Eds.), Tools for Constructing Chronologies: Crossing Disciplinary Boundaries. In: Lect. Notes Stat., vol. 177. Springer, New York, pp. 43–82.

Le Goff, M., Gallet, Y., 2004. A new three-axis vibrating sample magnetometer for continuous high-temperature magnetization measurements: applications to paleo- and archeointensity determinations. Earth Planet. Sci. Lett. 229, 31–43.

Licht, A., Hulot, G., Gallet, Y., Thébault, E., 2013. Ensembles of low degree archeomagnetic field models for the past three millennia. Phys. Earth Planet. Inter. 224, 38–67.

Livermore, P.W., Fournier, A., Gallet, Y., 2014. Core-flow constraints on extreme archeomagnetic intensity changes. Earth Planet. Sci. Lett. 387, 145–156.

Mitra, R., Tauxe, L., McIntosh, S.K., 2013. Two thousand year of archeointensity from West Africa. Earth Planet. Sci. Lett. 364, 123–133.

Muscheler, R., Beer, J., Kubik, P.W., Synal, H.-A., 2005. Quat. Sci. Rev. 24, 1849–1860.

Pavón-Carrasco, F.J., Gómez-Paccard, M., Hervé, G., Osete, M.L., Chauvin, A., 2014a. Intensity of the geomagnetic field in Europe for the last 3 ka: influence of data quality on geomagnetic field modeling. Geochem. Geophys. Geosyst. 15. http://dx.doi.org/10.1002/2014GC005311.

Pavón-Carrasco, F.J., Osete, M.L., Torta, J.M., De Santis, A., 2014b. A geomagnetic field model for the Holocene based on archaeomagnetic and lava flow data. Earth Planet. Sci. Lett. 388, 98–109. http://dx.doi.org/10.1016/j.epsl.2013.11.046.

Pick, T., Tauxe, L., 1993. Holocene paleointensities: Thellier experiments on submarine basaltic glass from the East Pacific Rise. J. Geophys. Res. 98 (B10), 17949–17964.

Prévot, M., Mankinen, E.A., Coe, R.S., Grommé, C.S., 1985. The Steens Mountain (Oregon) geomagnetic polarity transition. 2. Field intensity variations and discussion of reversal models. J. Geophys. Res. 90, 10417–10448.

Schnepp, E., Lanos, P., Chauvin, A., 2009. Geomagnetic paleointensity between 1300 and 1750 A.D. derived from a bread oven floor sequence in Lübeck, Germany. Geochem. Geophys. Geosyst. 10 (8), Q08003. http://dx.doi.org/10.1029/2009GC002470.

Shaar, R., Ben-Yosef, E., Ron, H., Tauxe, L., Agnon, A., Kessel, R., 2011. Geomagnetic field intensity: how high can it get? How fast can it change? Constraints from Iron Age copper slag. Earth Planet. Sci. Lett. 301, 297–306.

Shaar, R., Tauxe, L., Ben-Yosef, E., Kassianidou, V., Lorentzen, B., Feinberg, J.M., Levy, T.E., 2015. Decadal-scale variations in geomagnetic field intensity from ancient Cypriot slag mounds. Geochem. Geophys. Geosyst. 16 (1), 195–214. http://dx.doi.org/10.1029/2014GC005455.

Tema, E., Gómez-Paccard, M., Kondopoulou, D., Almar, Y., 2012. Intensity of the Earth's magnetic field in Greece during the last five millennia: new data from Greek pottery. Phys. Earth Planet. Inter. 202–203, 14–26.

Thébault, E., Gallet, Y., 2010. A bootstrap algorithm for deriving the archeomagnetic field intensity variation curve in the Middle East over the past 4 millennia BC. Geophys. Res. Lett. 37, L22303.

Thébault, E., et al., 2015. International geomagnetic reference field: the 12th generation. Earth Planets Space 67, 79.

Thellier, E., Thellier, O., 1959. Sur l'intensité du champ magnétique terrestre dans le passé historique et géologique. Ann. Géophys. 15, 285–376.